Mineralogical Magazine, February 2000, Vol. 64(1), pp. 11–18

Further study of the cation ordering in phengite 3*T* by neutron powder diffraction

A. PAVESE[1,2,*], G. FERRARIS[3], V. PISCHEDDA[3] AND P. RADAELLI[4,†]

[1] Dipartimento di Scienze della Terra, Università di Milano, Via Botticelli 23, I-20133 Milano, Italy
[2] National Research Council, CNR, Centro di Studio per la Geodinamica Alpina e Quaternaria, Via Mangiagalli 34, 20133 Milano, Italy
[3] Dipartimento di Scienze Mineralogiche e Petrologiche, Università di Torino, Via Valperga Caluso 35, I-10125 Torino, Italy
[4] ILL Facility, Institut Laue-Langevin, 38042 Grenoble, France

ABSTRACT

Phengite 3*T* (Dora-Maira massif, Italian western Alps), with chemical composition $K_{0.96}Na_{0.01}Al_{1.44}Mg_{0.56}(Si_{3.59}Al_{0.41})O_{10}(OH)_2$ has been investigated using powder neutron diffraction, at the ILL (Institut Laue-Langevin) Facility, on the D2B diffractometer. Data sets were collected at 293 and 873 K, and the present results are compared with those obtained previously using the time-of-flight (TOF) technique, on the same compound. In the octahedral sheet, Al tends to order into the *M*2 site, in accordance with the measurements mentioned above, whereas the Al/Si tetrahedral ordering we observe (i.e. Si fully into *T*1 site) is at variance with that determined previously. These discrepancies are ascribed to the presence of talc impurities in the sample used previously (~6 wt.%), which affected the results obtained.

KEYWORDS: neutron powder diffraction, phengite 3*T*, Dora-Maira, tetrahedral and octahedral order, Rietveld refinement.

Introduction

PAVESE *et al.* (1997) carried out a neutron powder diffraction experiment on Mg-rich phengite 3*T*, from the Dora-Maira massif (western Alps, Italy), by means of the time-of-flight (TOF) technique, on the high resolution powder diffractometer (HRPD) of the ISIS Facility, to determine, through Rietveld refinements, the Mg/Al and Al/Si distributions in the octahedral (*O*) and tetrahedral (*T*) sheets, respectively. Talc impurities were found to occur in the powdered sample used at ISIS (~6 wt.%) and were accounted for by performing multi-phase Rietveld treatments. The structure parameters of talc were kept fixed at the values determined by Perdikatsis and Burzlaff (1981), and only an overall atomic displacement parameter was refined, given that the amount of talc present was too small to attempt a full structure refinement, which would also have been hindered by the common occurrence of stacking faults and of cation replacements. Three points are to be emphasized: (1) the structural defects mentioned above depend strictly on the individual sample, and hence it is difficult to account for them; (2) it has been shown by HRTEM (Ferraris *et al.*, 1997) that nanometric oriented intergrowths of talc layers occur along the stacking sequence of phengite 3*T* from the Dora Maira Massif and diffract coherently with the host matrix; these intergrowths could not be revealed easily by powder diffraction. We stress that the occurrence of talc intergrowths is not to be mistaken for the presence of a separate talc-phase, which, in contrast, would provide a normal powder pattern. (3) While the contribution to the diffraction signals from the tetrahedral (*T*) sheets of talc is very similar to that of phengite, because

* E-mail: pavese@p8000.terra.unimi.it
† Present address: ISIS Facility, Rutherford Appleton Laboratory, Chilton-Didcot, Oxon OX11 0QX, UK

of the modest Al content in the latter, the octahedral (*O*) sheets provide distinct contributions, as Mg and Al are major octahedral cations in talc and phengites, respectively.

Pavese *et al.* (1997) mentioned difficulties with their refinements, and were forced to introduce constraints based on previously-determined XRD *T*–*O* bond lengths (Amisano-Canesi *et al.*, 1994). This approach, along with the three factors mentioned above, might distort the final results.

As a talc-free sample of phengite 3*T* from the Dora-Maira massif became available, new neutron powder diffraction data collections at ambient conditions (RT) and at high temperature (HT) were carried out at ILL (Grenoble, France), on the high resolution D2B diffractometer, in order to provide a check on the conclusions drawn from the previous experiment.

The new results are presented in this paper and compared with the earlier findings, in the light of a critical analysis on the reliability of the partitioning determined by Rietveld refinement.

Experimental

Approximately 3 cm^3 of phengite 3*T* from the Dora-Maira massif were used for the present experiment, after grinding to 20–40 μm grain size. Chemical analyses, performed by means of an SEM Cambridge S-360, equipped with an EDS 860 Link-System, confirmed those reported previously by Pavese *et al.* (1997), and the resulting composition is $K_{0.96}Na_{0.01}Al_{1.44}Mg_{0.56}(Si_{3.59}Al_{0.41})O_{10}(OH)_2$. The neutron diffraction data collections were carried out with λ= 1.594 Å [Ge (115)], and with an effective resolution of $\Delta d/d \approx 10^{-3}$. The high intensity collection mode was chosen, as it made it possible to improve the counting statistics, without seriously degrading the resolution. The collection bank was equipped with 64 ^{3}He detectors, spanning 140°2θ-range, and spaced at 2.5° intervals. High temperature was achieved by a vanadium-element resistance furnace, and maintained constant by an ILL-developed controller. The thermal gradient, between the top and bottom of the V-can, was controlled so as not to exceed 2 K. Two data collections were performed, at ambient conditions and at 873 K, respectively, taking 24 h each. The pattern recorded at room temperature is shown in Fig. 1. The GSAS software package (Larson and Von Dreele, 1986) was used to perform the Rietveld refinements. A gaussian-like profile function, with asymmetry (Asy) and preferred orientation (PO) according to Howard (1982) and Dollase (1986), respectively, proved to be successful for modelling the diffraction patterns, and the FWHM was expressed using the parameters $\sigma^2 = \sigma_0 + \sigma_1 \tan(\theta) + \sigma \tan(\theta)^2$. The Asy and σ^2 coefficients were allowed to vary in both HT and RT refinements; PO was determined from the RT data, and its value was kept fixed during the treatment of the HT data sets. The following neutron scattering lengths from the database of the GSAS program were used in the refinements: Mg = 0.538, Al = 0.345, Si = 0.415, O = 0.581, H = −0.374, K = 0.367 10^{-12} cm.

Results and discussion

Site compositions

Structure refinements in the space group $P3_112$, by means of the Rietveld method, were carried out unconstrained, but we needed to conserve the chemical composition and full occupancies of the *M* and *T* sites. Cations were partitioned in order to fill the tetrahedral sheet with Si and Al, and the remaining Al, along with Mg, was distributed over the octahedral sheet into the *M* sites. In Fig. 2*a,b* the T-O-T layer (tetrahedral sheet-octahedral sheet-tetrahedral sheet) of phengites and the projection onto (001) plane of the octahedral sheet are displayed; the independent *T* sites (*T*1 and *T*2) and *M* sites (in dioctahedral micas, *M*2 and *M*3 are occupied, while *M*1 is empty) are shown. The *T* and *M* site cation distributions are fully determined by two degrees of freedom, which for convenience, we have chosen as the occupancy factors of Al in *M*2 (η_M) and of Si in *T*1 (η_T). The coordinates, and the AtDPs (Atomic Displacement Parameter; henceforth AtDP is meant as the 'isotropic AtDP', and *U(X)* indicates the AtDP of the *X* site) of the atoms were allowed to vary, using the structural parameters from Pavese *et al.* (1997) as starting values for the present refinements. Correlation effects, which can affect quantities such as η_T and η_M, were limited by grouping and refining separately the structure parameters and η values and then at the final stage allowing them to vary collectively.

Three refinement schemes (S, S_o, S_tS_o) were used, to check the reliability of the η values determined. In Table 1, η_T, and η_M the mean tetrahedral and octahedral bond lengths, and the AtDPs of the *T* and *M* sites, are reported, from the RT and HT refinements. In the latter case, only

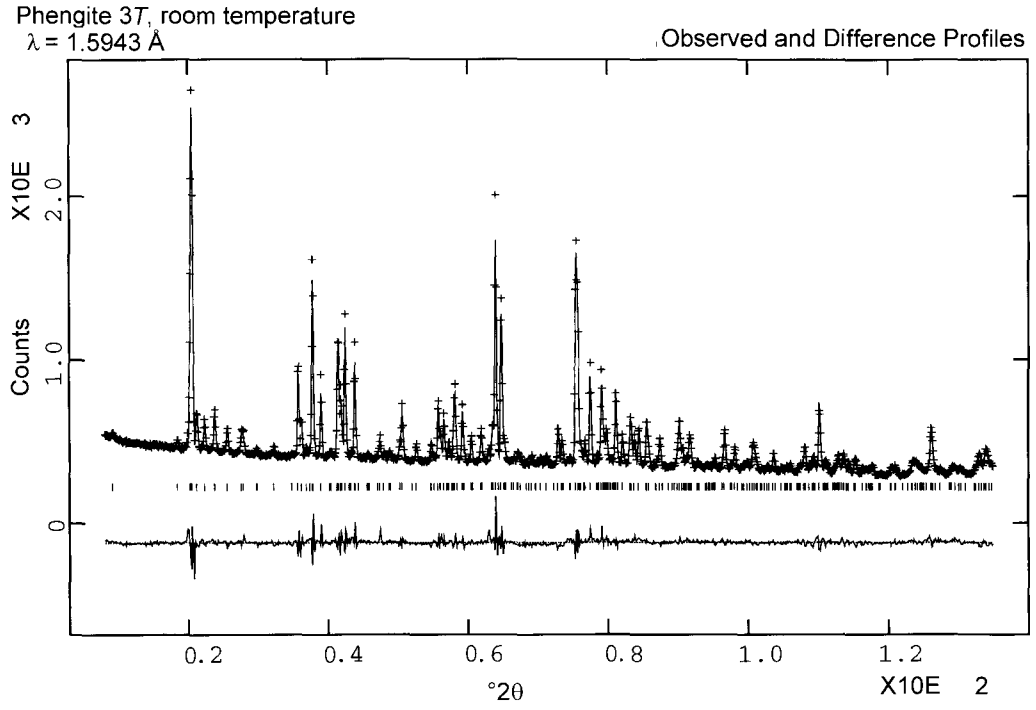

FIG. 1. Room temperature powder diffraction pattern of phengite 3*T*. The Obs−Calc difference is reported. Vertical bars mark the calculated peak positions.

the results from the S scheme are shown, as they are practically independent of the approach adopted.

The η_M was refined successfully from the ambient conditions data, and the three refinement schemes provided the results discussed below. The totally unconstrained scheme (S) yielded a very small thermal parameter for the *M*2 site, which could indicate the need to increase the Mg content of the *M*2 site, at the expense of Al. However, refinements performed with arbitrary octahedral cation distributions, ranging from total order to disorder, did not yield significantly larger *U*(*M*2). To explain the small *U*(*M*2) value one could invoke the occurrence of the aforementioned nanometric talc intergrowths, which might decrease *U*(*M*2) on account of an excess of scattering power from the *O* sheets, due to Mg coherently diffracting in the talc-like layers. We do not observe a similar effect with the AtDPs of the *T* sites because the neutron scattering length of the tetrahedral talc-sheets filled by Si is only comparable with that of the tetrahedral sheets of our sample, wherein 0.4 Al *vs* 3.6 Si atoms are distributed over four *T* sites.

In the S_o scheme, the *M*2 and *M*3 site AtDPs were constrained to be equal to each other, whereas in S_tS_o the constraint *U*(*T*1) = *U*(*T*2) was also added. Such constraints are justified by the fact that *T*1 and *T*2 (*M*2 and *M*3) are expected, on the basis of the results from single crystal XRD studies (Amisano-Canesi *et al.*, 1994), to have similar AtDPs.

The η_M ranges from 0.86(5) to 0.96(6), and its variation is largely correlated with the use of constrained octahedral AtDPs, as shown in Table 1. However, taking into account that an ideally disordered *M* partitioning would require η_M = 0.72, the results above suggest the tendency of Al to order into the *M*2 site.

The refinement of η_T required a less straightforward treatment. In fact, the effective tetrahedral site neutron scattering lengths were refined under the constraint that the total neutron scattering length in the *T* sheet was conserved. The Al/Si partitioning was subsequently derived, taking into account that each site neutron scattering length is the linear combination of the individual neutron scattering lengths of Al and Si according to the site composition. Following this procedure we

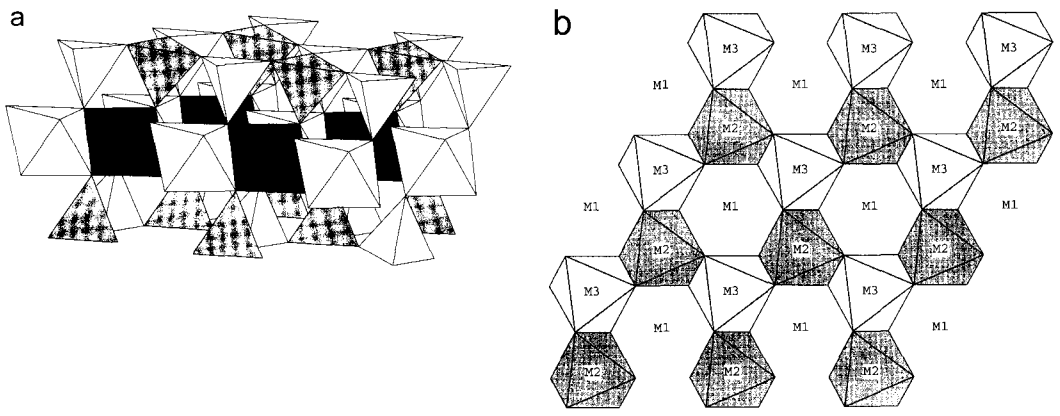

FIG. 2. (*a*) The T-O-T layer is shown. *T*1 and *T*2, which are the independent sites in the tetrahedral sheet, correspond to white and grey tetrahedra, respectively. The independent sites of the octahedral sheet are *M*2 (white) and *M*3 (grey). (*b*) Projection onto (001) plane of the octahedral sheet of dioctahedral micas. The independent sites [*M*1 (empty), *M*2 (filled) and *M*3 (filled)] are displayed.

obtained, independently of the refinement scheme adopted, an excess of Si, in *T*1, algebraically compensated by a negative occupancy factor of Al, which in turn, overfilled *T*2, with negative Si occupancy. Although this result is non-physical, it indicates that the *T*1 site requires such a large neutron scattering length that it can be attained just by fully hosting Si (see the neutron scattering length values reported above). Hence, the *T*1 site was constrained to contain Si only, and the composition of *T*2 was derived accordingly. Table 1 reveals the mean $T1-O$ bond length is less than that for $T2-O$, in accordance with the partitioning determined. The refined content of Al in the *T*2 site (0.21 atoms per site) is not far from that inferred by the equation of Hazen and Burnham (1973), predicting 0.24 on the basis of the bare tetrahedral mean bond distances.

η_T and η_M, refined from the high temperature data, did achieve convergence but led to Si- and Al-oversaturation of the *T*1 and *M*2 sites, respectively. This suggests, on the basis of the arguments adopted above for the RT refinement, that Si and Al maintain their tendency to order into *T*1 and *M*2 sites, even upon heating.

The value of *U*(*M*2) is reasonable at high temperature, although the talc-intergrowths, used to explain the abnormal *U*(*M*2) value determined at RT, must still be present. Presumably the thermal motion increase caused by heating swamps the effects of 'static' origin, due to the talc intergrowths. In turn, the reliability of the site occupancies should be guaranteed by (1) the precautions adopted in the refinements, as stated above, and (2) by the neutron scattering lengths being independent of $\sin(\theta)/\lambda$, which limits the correlations between AtDPs and η^- values.

The average tetrahedral bond lengths are similar at high temperature to the RT-results, in accordance with the generally-observed thermal inertness of tetrahedra in silicates. This result is a further hint that no cation rearrangement occurs upon heating, since, in the case of phengite $2M_1$, which actually suffers an order/disorder reaction at HT (Pavese *et al.*, 1999), a significant change of the Si–O mean bond lengths takes place with increasing temperature. A detailed analysis of the $T-O$ bond lengths shows that they range from 1.58(1) to 1.66(1) Å at RT, and from 1.60(1) to 1.69(2) Å at HT, whereas $T2-O$ bond lengths range from 1.61(2) to 1.67(1) Å at RT, and from 1.49(2) to 1.74(1) Å at HT. The unrealistic range of $T2-O$ and the increase of distortion upon heating can be explained as follows: (1) the use of isotropic rather than anisotropic thermal parameters might distort the geometrical features of the structure, particularly in the high temperature regime, by shifting the atomic barycentres of vibration (i.e. atomic positions); (2) the site most markedly exhibiting anomalous bond length behaviour is *T*2, in agreement with the conclusions from the site-occupancy refinement which indicates *T*2 as the site containing both Si and Al, and therefore more likely affected by strain.

TABLE 1. $T-O$ and $M-O$ average bond lengths (Å), η_T (Si content at $T1$) and η_M (Al content at $M2$) coefficients, and AtDPs (Å^2 × 100) of the tetrahedral and octahedral sites from the Rietveld refinements at 293 K (a) and 873 K (b). S is defined in the text. $R = \Sigma I_{obs} - I_{calc} / \Sigma I_{obs}$, $wR_p = \Sigma I_{obs} - I_{calc} w / \Sigma I_{obs} w$, where I indicates the intensities of each profile point, and w the corresponding weights, calculated as $1/\sigma(I)^2$

Temperature = 293 K			
Refinement scheme	S	S_o	S_tS_o
η_M	0.96(6)	0.86(5)	0.85(4)
η_T	1.0	1.0	1.0
U(M2)	0.1(3)	1.0(1)	1.0(1)
U(M3)	1.8(3)		
U(T1)	1.6(3)	1.7(3)	1.44(9)
U(T2)	1.1(3)	1.0(3)	
<*M2*–*O*>	1.966(8)	1.967(8)	1.967(8)
<*M3*–*O*>	1.954(8)	1.952(8)	1.951(8)
<*T1*–*O*>	1.631(8)	1.629(8)	1.628(8)
<*T2*–*O*>	1.641(8)	1.644(8)	1.645(8)
$R_p \times 100$	2.74	2.75	2.75
$WR_p \times 100$	3.98	3.98	3.99
Temperature = 873 K			
η_M	1.0		
η_T	1.0		
U(M2)	2.2(4)		
U(M3)	1.8(3)		
U(T1)	1.9(2)		
U(T2)	3.5(3)		
<*M2*–*O*>	1.963(9)		
<*M3*–*O*>	1.978(8)		
<*T1*–*O*>	1.637(8)		
<*T2*–*O*>	1.641(9)		
$R_p \times 100$	2.74		
$WR_p \times 100$	3.74		

With regard to the $M-O$ bond lengths, $M2-O$ does not change whereas the length of $M3-O$ increases. This is consistent with the fact that the mean bond length thermal expansion coefficients of octahedrally-coordinated Al and Mg are 8×10^{-6} and $14 \times 10^{-6} K^{-1}$ respectively (Yamanaka and Takeuchi, 1983), and we could expect the Al–filled $M2$ site to expand less than the $M3$ site, wherein Mg orders. Therefore, the behaviour of the average $M-O$ bond length supports the theory of the cation ordering inferred from the refinements of the site occupancy factors.

The results in Table 1 may be interpreted in the following ways.

(1) If the S_o or S_tS_o schemes are accepted for the RT refinement, an order-disorder reaction should take place at HT, causing Al to fully enter the $M2$ site, with displacement of Mg to $M3$. The occurrence of such a process would be in agreement with the contraction of $M2-O$ and the lengthening of $M3-O$ upon heating. However, such a cation readjustment would only cause slight changes of composition on the M sites, ~0.15 atoms per site, considering that the uncertainty is 0.05 atoms per site.

(2) If the S scheme is used, no cation exchange between $M2$ and $M3$ occurs, and any interatomic bond length is due entirely to thermal effects.

Whichever account one accepts, the essence of the results reported is that Al tends to order into the $M2$ sites, in the O sheet, while Si occupies the $T1$ site, in the O sheet, and this partitioning is largely preserved upon heating.

In Table 2 the structure parameters refined at ambient conditions and at high temperature are reported.

TABLE 2. (*a*) Cell parameters (Å), structure and preferred orientation parameters (PO) refined from room temperature data.

	x	*y*	*z*	$U_{iso} \times 100$
K	0.124(2)	0.248(3)	1/6	20.5(3)
M2	0.799(3)	0.899(1)	0	00.1(3)
M3	0.441(3)	0.221(2)	0	10.8(4)
T1	0.791(2)	0.581(3)	0.0897(7)	1.6(3)
T2	0.462(2)	0.916(2)	0.0907(6)	1.1(3)
O1	0.749(3)	0.563(2)	0.0355(5)	1.4(2)
O2	0.499(2)	0.940(1)	0.0368(5)	1.3(2)
O3	0.652(2)	0.772(2)	0.1139(4)	1.7(2)
O4	0.122(2)	0.714(2)	0.1065(4)	1.3(2)
O5	0.606(2)	0.252(2)	0.1139(5)	1.7(2)
O6	0.127(2)	0.196(2)	0.0351(3)	2.2(2)
H	0.155(3)	0.392(3)	0.0363(6)	3.3(3)
PO	1.690(1)			
a	5.215(1)			
c	29.745(3)			

TABLE 2. (*b*) Cell parameters (Å), structure and preferred orientation parameters (PO) refined from high temperature data

	x	*y*	*z*	$U_{iso} \times 100$
K	0.129(3)	0.258(6)	1/6	7.8(5)
M2	0.789(4)	0.895(2)	0	2.2(4)
M3	0.455(3)	0.228(2)	0	1.8(3)
T1	0.792(2)	0.583(3)	0.0931(5)	1.9(3)
T2	0.453(3)	0.901(3)	0.0857(6)	3.5(3)
O1	0.742(2)	0.563(2)	0.0372(5)	2.8(2)
O2	0.495(2)	0.939(2)	0.0366(5)	2.2(2)
O3	0.657(2)	0.774(2)	0.1145(4)	3.0(2)
O4	0.131(2)	0.722(1)	0.1074(5)	2.7(1)
O5	0.632(2)	0.244(2)	0.1105(6)	3.2(2)
O6	0.112(2)	0.188(2)	0.0338(4)	3.3(3)
H	0.150(5)	0.384(4)	0.039(1)	8.8(6)
a	5.233(1)			
c	30.134(3)			

Hydroxyl group

The position of the H atom was refined successfully both from the room temperature (O–H = 0.96(1) Å) and from the high temperature (OH = 0.96(2) Å) data collections. The hydroxyl bond length does not suffer significant change, whereas the inclination angle of OH towards (001) cleavage plane shifts from 2°, at RT, to 9° at HT. This is probably due to the increasing importance of the vibrational energy component, upon heating, which entails larger H vibrations. Hydrogen moves farther from the (001) plane and approaches the ideally hexagonal cavity of the tetrahedral sheet, in order to have room to vibrate. This geometrical configuration of the hydroxyl group fulfils those requirements pointed out by Ferraris *et al.* (1995) to reduce the effects of repulsion, which would contribute, along with the cation arrangements in the octahedral and tetrahedral sheets, to stabilize the 3*T* phase at high pressure.

Comparison with results from previous measurements

The results reported here are in agreement with those from Pavese *et al.* (1997), as far as the octahedral cation partitioning is concerned, whilst they are at variance with regard to the Al/Si tetrahedral distribution. The T distribution we determined here is the reverse of that proposed by Pavese *et al.* (1997), who suggested that tetrahedral Al orders into the $T1$ site. This discrepancy can be ascribed to the presence of talc impurities, in the sample studied previously, which made it necessary to constrain the $T-O$ and $M-O$ bond lengths to their values from an earlier investigation (Amisano-Canesi *et al.*, 1994).

Both our results and those from Pavese *et al.* (1997) support the hypothesis of energetically non-equivalent $T1$ *vs* $T2$ and $M2$ *vs* $M3$ sites, thus favouring ordered distributions. This is in keeping with the fact that the $3T$ polytype formed at high pressure conditions, within an environment dominated by baric effects. These condition can promote crystallization of minerals with ordered cation distribution to minimize the Gibbs energy, by exploiting energetically non-equivalent sites (see the discussion on the role of the static energy at high pressure conditions in Wentzcovitch and Stixrude, 1997). The present results and those of Pavese *et al.* (1997) agree that the cation partitioning inferred from the room temperature refinements is preserved upon heating. This fact supports the energetic non-equivalence of the $T1$/$T2$ and $M2$/$M3$ sites, which exhibit remarkable preference to host specific chemical species.

Energy calculations would produce distorted results in predicting the stability field of polytype $3T$, if the incorrect partitioning reported by Pavese *et al.* (1997) was used. The force fields warranting the stability of structures are a sensitive function of the cation ordering, and the use in calculations of an incorrect atomic distribution causes failure in evaluating both static and vibrational energy (Vieillard, 1995).

The results obtained for $3T$ differ from those for $2M_1$ Fe-rich phengites (Pavese *et al.*, 1999), where tetrahedral order is observed only upon heating. The peculiar behaviours of these micas presumably reflect different energetics and structural details of the TOT layer in $3T$ and $2M_1$ polytypes, which display C12(1) and C$\bar{1}$ TOT layer symmetry, respectively, though the ideal layer symmetry is, in both cases, $C12/m(1)$ (Nespolo *et al.*, 1997).

The cell parameters we obtained from the present measurements (Table 2a,b) are consistent with the thermal expansion coefficients determined by Pavese *et al.* (1997).

Conclusions

The following conclusions can be drawn.

(1) At ambient conditions, both tetrahedral and octahedral cations show ordered distributions; Al exhibits preference for the $M2$ site, in the octahedral sheet, whereas Si enters the $T1$ site, in the tetrahedral sheets.

(2) The cation partitioning at room temperature does not change upon heating.

These conclusions, agree with those from Pavese *el al.* (1997), in relation to octahedral distribution and the preservation of the cation ordering with increasing temperature. They are at variance in relation to the tetrahedral cation partitioning: the results here are the reverse of those in the Pavese *et al.* (1997) paper. We consider the present results to be more reliable because of the greater purity of the sample used.

Acknowledgements

The authors thank Martin Dove and two anonymous referees for comments and suggestions which improved the manuscript. This work was supported financially by CNR and MURST ('Relationships between structure and properties in minerals: analysis and applications' project) grants, and by the 'Centro di studio per la geodinamica alpina e quaternaria' (Milano) and 'Centro di studio sulla geodinamica delle catene collisionali' (Torino). Provision of neutron scattering facilities by the Institut Laue Langevin (ILL) is gratefully acknowledged.

References

Amisano-Canesi, A., Chiari, G., Ferraris, G., Ivaldi, G. and Soboleva, V.S. (1994) Muscovite and phengite 3T: crystal structure and conditions of formation. *Eur. J. Mineral.*, **6**, 489–96.

Dollase, W.A. (1986) Correction of intensities for preferred orientation in powder diffractometry: application of the March model. *J. Appl. Cryst.*, **19**, 267–72.

Ferraris, C., Lanfranco, A.M. and Hiltunen, R. (1997) Polytypism and non periodic interstratifications in some alpine micas: HRTEM and multiphase carbon detector data. *MODUL 97-Modular Aspects of Minerals, Abstracts*. 1st EMU School and Symposium. Budapest, Hungary, p. 19.

Ferraris, G., Ivaldi, G., Nespolo, M. and Takeda, H. (1995) On the stability of dioctahedral micas. *Terra Abstr. (Suppl. No. 1, Terra Nova)*, **7**, 289.

Hazen, R.M. and Burnham, C.W. (1973) The crystal structure of one layer phlogopite and annite. *Amer. Mineral.*, **58**, 889–900.

Howard, C.J. (1982) The approximation of asymmetric neutron powder diffraction peaks by sums of gaussians. *J. Appl. Crystallogr.*, **15**, 615–20.

Larson, A.C. and Von Dreele, R.B. (1986) *GSAS: General Software Analysis System Manual.* Los Alamos National Laboratory Report. LAUR: 86–87.

Nespolo, M., Takeda, H. and Ferraris, G. (1997) Crystallography of mica polytypes. Pp. 81–118 in: *Modular Aspects of Minerals* (S. Merlino, editor). EMU Notes in Mineralogy, **1**.

Pavese, A., Ferraris, G., Prencipe, M. and Ibberson, R. (1997) Cation site ordering in phengite 3T from the Dora Maira massif (western Alps) a variable-temperature neutron powder diffraction study. *Eur. J. Mineral.*, **9**, 1183–90.

Pavese, A., Ferraris, G., Pischedda, V. and Ibberson, R. (1999) Tetrahedral order upon heating in phengite $2M_1$, from powder neutron diffraction. *Eur. J. Mineral.*, **11**, 309–20.

Perdikatsis, B. and Burzlaff, H. (1981) Strukturverfeinerung am Talc Mg_2 $[(OH)_2Si4O_{10}]$. *Zeits. Kristallogr.*, **156**, 177–86.

Vieillard, Ph. (1995) How do uncertainties of structure refinements influence the accuracy of the prediction of enthalpy of formation? Examples on muscovite and natrolite. *Phys. Chem. Min.*, **22**, 428–36.

Wentzcovitch, R.M. and Stixrude, L. (1997) Crystal chemistry of forsterite: a first principles study. *Amer. Mineral.*, **82**, 663–71.

Yamanaka, T. and Takeuchi, Y. (1983) Order-disorder transition in $MgAl_2O_4$ spinel at high temperature up to 1700°C. *Zeits. Kristallogr.*, **165**, 65–78.

[*Manuscript received 10 November 1998: revised 18 May 1999*]